

## Generation of Red Light Femtosecond Pulses from an Intra-Cavity Frequency-Doubled Cr<sup>4+</sup>: Forsterite Laser \*

ZHONG Xin(钟欣), ZHOU Bin-Bin(周斌斌), ZHAN Min-Jie(詹敏杰), WEI Zhi-Yi(魏志义)\*\*

Beijing National Laboratory for Condensed Matter Physics, Institute of Physics, Chinese Academy of Sciences, Beijing 100190

(Received 9 October 2009)

We demonstrate the generation of red light femtosecond laser pulses from an intra-cavity frequency-doubled Cr<sup>4+</sup>:forsterite laser. Average output power of 75 mW is obtained at the central wavelength of 647 nm with pulse width of 55 fs by inserting a 500- $\mu$ m-thick BBO crystal in the laser cavity. The bandwidth of spectrum of second harmonic pulses is 9 nm, corresponding to a time-bandwidth product of 0.355.

PACS: 42.55. -f, 42.65. Ky, 42.65. Re

DOI: 10.1088/0256-307X/27/4/044204

Femtosecond laser pulses in red light are attractive for their most wide applications in ultrafast dynamics research and the promising use in remote sensing,<sup>[1]</sup> medicine,<sup>[2]</sup> two-photon laser microscopy,<sup>[3]</sup> etc. Conventional laser sources at this wavelength range are the well developed dye lasers. By changing the gain material, the output wavelength from dye lasers can be tuned. However, the dye lasers perform obvious drawbacks such as the relatively short working time for periodic dye change, environment noise, low output power and harmful character. Although femtosecond Ti:sapphire lasers show excellent performance as a revolutionary ultrafast laser source, it cannot cover some important wavelength range in red light. Optical parametric oscillators (OPOs) pumped by the frequency doubled femtosecond Ti:sapphire lasers, which have been demonstrated by a few groups,<sup>[4,5]</sup> are possible solution to cover the gap for ultrafast phenomena applications. However, the OPOs remain complicated technology, poor stability, low output power and high cost.

Cr<sup>4+</sup>:forsterite crystal has luminescence spectrum from 1100 nm to 1500 nm<sup>[6]</sup> and typically works with laser output wavelength between 1200 nm and 1350 nm. Femtosecond laser pulses in red light can be obtained by frequency doubling the mode-locked Cr<sup>4+</sup>:forsterite laser. Sennaroglu *et al.*<sup>[7]</sup> reported generation of 116 fs pulses at 615 nm in a LiIO<sub>3</sub> with conversion efficiency approaching 10%; efficient generation of 50-fs pulses at 620 nm in an LBO crystal with conversion efficiency up to 44% was obtained by Liu *et al.*<sup>[8]</sup> Yanovsky *et al.* obtained 100-fs pulses at 625 nm with conversion efficiency as high as 53% through an external-enhancement cavity.<sup>[9]</sup> Typically there are three kinds of frequency doubling schemes, namely external-one-pass, external-enhancement-cavity and intra-cavity. For the external-one-pass scheme, it is not very suitable for the direct generating of second

harmonic of an oscillator due to the low pulse energy, which results in a relatively low conversion efficiency. For the enhancement-cavity scheme, the conversion efficiency may be highly increased, but a complex configuration and rigorous alignment are necessary. Compared with the above schemes, intra-cavity frequency doubling is a better choice due to the advantages of high efficiency and relatively simple configuration.

Previously we reported an efficient mode-locked Cr<sup>4+</sup>:forsterite oscillator.<sup>[10]</sup> As a subsequent work, in this study we demonstrate intra-cavity frequency doubling of this oscillator with some modification to the cavity configuration. A 500- $\mu$ m-thick BBO is used as the frequency doubling crystal. Output power of 75 mW is obtained at the central wavelength of 647 nm. Autocorrelation measurements show that widths of fundamental and second harmonic pulses are 43 fs and 55 fs, respectively, after inserting BBO crystal.

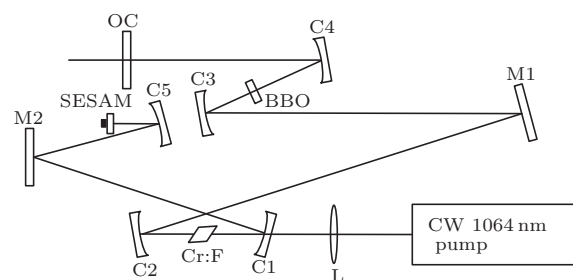


**Fig. 1.** Schematic diagram of the experimental setup. L: lens with focal length of 100 mm; C1-C5: concave mirrors with ROC of 100 mm.

The schematic diagram of the experimental setup is shown in Fig. 1. The Cr<sup>4+</sup>:forsterite crystal has a dimension of 4 × 2 × 9 mm<sup>3</sup>, cut for propagation along the *a*-axis and emitting beam polarization along the *c*-axis. End faces are Brewster cut and polished. Ow-

\*Supported by the National Natural Science Foundation of China under Grant Nos 10874237 and 10704087, the National Basic Research Program of China under Grant Nos 2007CB815104, and the Knowledge Innovation Program of Chinese Academy of Sciences.

\*\*Email: wzhy@aphy.iphy.ac.cn

© 2010 Chinese Physical Society and IOP Publishing Ltd

ing to the poor thermal conductivity,<sup>[11]</sup> the forsterite crystal is wrapped in an indium foil and mounted in a copper holder, which is clamped on the cold side of a thermoelectric cooler (TEC). When laser running, the crystal is kept at the temperature near 0°C. Astigmatism compensation is applied by choosing the incidence angle at 11° on both the concave mirrors C1 and C2.<sup>[12]</sup> All the mirrors used are highly reflectively coated from 1150 nm to 1350 nm except the OC with transmission rate of 2.5%. In addition, both C1 and C2 are also dichromatically coated for anti-reflection (AR) at 1064 nm. Utilizing the formula in Ref. [13], we calculate the group-delay-dispersion (GDD) in Cr<sup>4+</sup>:forsterite to be 16.33 fs<sup>2</sup>/mm at 1300 nm. For the crystal length of 9 mm, the total positive GDD is 147 fs<sup>2</sup> per pass. In order to compensate the dispersion, we introduce six chirped mirrors. Each bounce on C1, C2, C3 and C4 brings GDD of  $-60 \pm 20$  fs<sup>2</sup> and  $-70 \pm 20$  fs<sup>2</sup> on M1 and M2, respectively, so that the total net second order dispersion in the cavity is about  $-233$  fs<sup>2</sup> per pass. Due to the unpredictable small oscillations in the GDD introduced by the six chirped mirrors, more negative GDD is necessary for keeping the net dispersion within the whole spectrum range to be negative, which is very important for stable mode-locking. According to our cavity configuration, the second harmonic generation (SHG) output comes out from C3, C4 and OC. The transmissivity of both C3 and C4 is about 64% near 647 nm and about 48% for OC, respectively. The incidence angles on C3 and C4 are as small as possible for keeping good beam quality. The commercial SESAM (BATOP GmbH) has a modulation depth of 2.5% at central wavelength of 1300 nm, saturation fluence of 70 μJ/cm<sup>2</sup> and nonsaturable loss less than 0.5%. Among kinds of nonlinear material such as LiIO<sub>3</sub>, LiNO<sub>3</sub>, LBO, KTP and BBO, we choose BBO as the frequency doubling crystal for its relatively large nonlinear coefficient, small GDD at wavelength of 1300 nm and good quality based on mature growing technique. Meanwhile, the GVM between fundamental wave and SHG in BBO can be obtained from Eqs. (1) and (2), which turns out to be 0.0268 mm/fs. As a result, the characteristic length of 1.34 mm can be obtained by Eq. (3).<sup>[14]</sup> In order to avoid efficient pulse broadening,<sup>[15,16]</sup> we choose the length of BBO to be 500 μm, shorter than half of characteristic length. The 500-μm-thick BBO crystal is cut for type-I (o+o->e) frequency doubling of 1290 nm ( $\theta = 20.6^\circ$ ,  $\phi = 0^\circ$ , FuJian Castech Crystal INC.) and AR coated for both fundamental and second harmonic waves,

$$v_G = c \left( n - \lambda \frac{dn}{d\lambda} \right)^{-1}, \quad (1)$$

$$\text{GVM} = \left( \frac{1}{V_{G,\text{FUN}}^o} - \frac{1}{V_{G,\text{SHG}}^e} \right)^{-1}, \quad (2)$$

$$L_c = \tau_p / |\text{GVM}^{-1}|. \quad (3)$$

A commercial cw Yb-doped fiber laser (AYDLS-PM-10, Amonics) working at 1064 nm is used as the pump source. It can deliver maximum power of 7.9 W. Without inserting the BBO crystal, maximum stable mode-locked output power of 320 mW is obtained under pump power of 6.9 W by optimizing the distance between C1 and C2, the displacement of forsterite crystal, the distance between C3 and C4 as well as the beam waist on SESAM. The total cavity length of the oscillator is 1870 mm, corresponding to the repetition rate of 80 MHz.

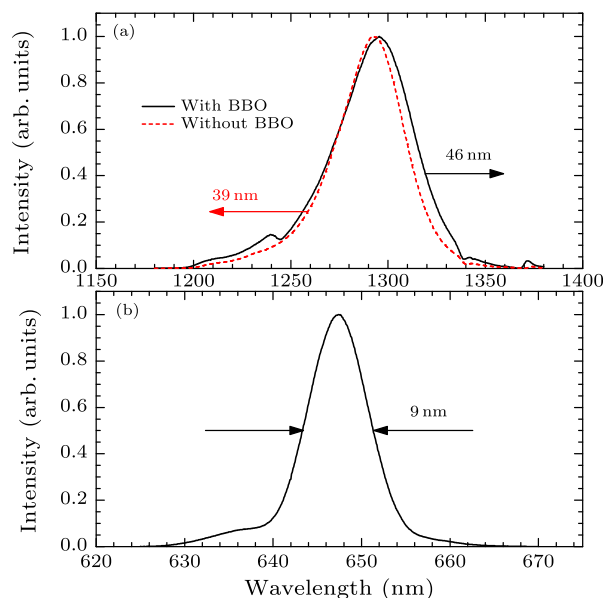


**Fig. 2.** (a) Without BBO inserted, the spectrum of fundamental wave is centered at 1292 nm with FWHM of 39 nm (black line); with BBO inserted, the spectrum center red shifts to 1295 nm with FWHM of 46 nm (red line); (b) the spectrum of SHG is centered at 647 nm with FWHM of 9 nm.

In order to obtain higher power density to enhance the nonlinear effect in BBO crystal, C3 and C4 form another focal spot inside the cavity. Then we directly insert the thin BBO crystal perpendicularly to the beam into the cavity. The insertion point is crucial because only within a certain range can the oscillator keep stable mode-locking. For example, the insertion point should not be right at the focal point. Although the higher power density at focal point is helpful for high conversion efficiency, much depletion of fundamental wave may lead to unstable mode-locking. For this reason, we optimize the best insertion point by monitoring the SHG power with a power meter (407A, Spectra-Physics INC.) and the fundamental spectrum with a spectra analyzer (AQ-6315A, ANDO). By slightly moving the BBO and rotating its horizontal angle, we stably realize the efficient red light emission. Figure 2 shows the spectrum of both fundamental wave and SHG, from which we can see the spectrum of the fundamental pulse is broadened a little after BBO inserted, which we at-

tribute to the self-phase-modulation (SPM) effect in the BBO crystal. By rotating the horizontal angle of BBO crystal, we observe the shift of central wavelength, shown in Fig. 3. We think that two reasons mainly contribute to the wavelength shift. First, the phase-matching condition varies when the horizontal angle changes. Second, the reflection of coatings on surfaces of BBO will also vary a little with the change of incident angle, as explained in Ref. [17].

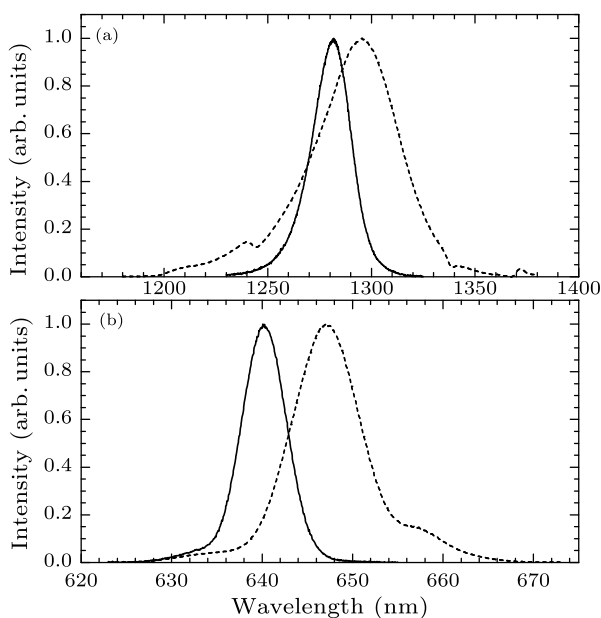


**Fig. 3.** The BBO angle tuning of fundamental wave and SHG wavelength. (a) The central wavelength of fundamental wave can be tuned from 1280 nm (solid line) to 1296 nm (dashed line). (b) SHG central wavelength from 640 nm (solid line) to 648 nm (dashed line).

We measure the pulse width with a commercial intensity autocorrelator (FemtoChrome FR-103MN). The intensity autocorrelation traces of fundamental and SHG before/after BBO inserted are shown in Fig. 4. The duration of fundamental pulses becomes a bit shorter after BBO inserted. The BBO only brings GDD of  $8\text{ fs}^2$  to the fundamental wave, which can be neglected for pulse broadening. Thus the shortening of pulse duration shows consistency with the spectrum broadening mentioned before. The time-bandwidth products are 0.343 (fundamental without BBO), 0.353 (fundamental with BBO) and 0.355 (SHG), respectively.

To measure the threshold power of the oscillator with BBO inserted, we increase the pump power from very low level. When the pump power reaches to 4 W, the oscillator starts to have cw fundamental output. The evolution of mode-locking is monitored by a spectra analyzer and a photodiode. Figure 5 shows the output power at different situations, which we summarize as three regions with pump power increasing. In region I, the laser performs only with cw output. Neither mode-locking operation nor even weak cw red

light is observed because of lower power in the cavity. The data only represents the power of fundamental wave. In region II, the laser runs in good mode-locking state. Efficient generation of SHG is obtained. The data shows the total SHG output by filtering the fundamental wave. In fact, between regions I and II, there is a very small region in which the oscillator works under unstable mode locking state but still has weak red light output. In region III, the mode-locking becomes unstable again, mainly caused by the increase of thermal lens effect in forsterite crystal under the high pump power, resulting in the decrease of SHG power. Under the optimized running state, we measure the SHG power to be 15 mW from OC, 24 mW from C3 and 36 mW from C4, respectively, which is 75 mW in total.

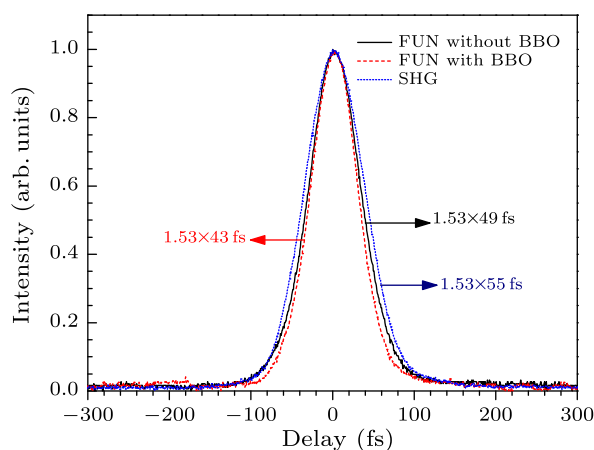


**Fig. 4.** Autocorrelation traces of fundamental wave and SHG pulses. Fundamental wave without BBO inserted (black line); fundamental wave with BBO inserted (red line); SHG wave (blue line).

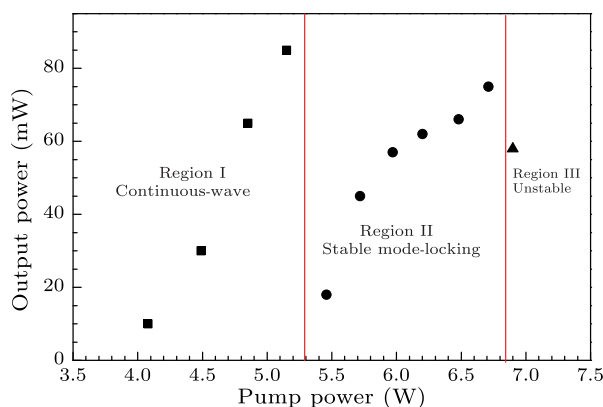


**Fig. 5.** Variation of output power vs pump power. Region I: cw output power of fundamental wave (filled square). Region II: Total SHG power of stable mode-locking (filled circle). Region III: Power of SHG., unstable mode-locking causes the decrease of SHG output power (filled triangle).

The mode locking SHG performs stably during the observing time. Within 1.5 hours, the power of red light out from C4 keeps near the average value of 30 mW and varies within  $\pm 3\text{ mW}$ , which corresponds

to a power uncertainty of  $< 10\%$ . However, the water condensation on copper holder or even the crystal surfaces sometimes disturbs the mode-locking, especially in summer when it is relatively humid. We will employ the nitrogen blowing setup to solve this problem.

In conclusion, we have demonstrated an intracavity frequency doubled mode-locked  $\text{Cr}^{4+}$ : forsterite oscillator by inserting a BBO crystal with thickness of  $500\ \mu\text{m}$ . Stable laser pulses in red light centered at  $647\ \text{nm}$  with power of  $75\ \text{mW}$  are obtained. The pulse duration is as short as  $55\ \text{fs}$ , which is only 1.12 times of the transform limit. The output wavelength of fundamental and SHG can be slightly tuned by rotating the horizontal angle of BBO. The frequency doubled oscillator shows good stability under dry environment and can be used as a good femtosecond source of red light.

We thank Hao Teng, Hainian Han and Zhaohua Wan for helpful discussion.

## References

- [1] Curran P 1980 *Prog. Phys. Geograph.* **4** 315
- [2] Papageorgiou P, Katsambas A and Chu A 2000 *British J. Dermatology* **142** 973
- [3] Denk W, Strickler J H and Webb W W 1990 *Science* **248** 73
- [4] Ghotbi M, Esteban-Martin A and Ebrahim-Zadeh M 2006 *Opt. Lett.* **31** 3128
- [5] Gale G M, Cavallari M and Hache F 1998 *J. Opt. Soc. Am. B* **15** 702
- [6] Kuleshov N V et al 1997 *J. Lumin.* **75** 319
- [7] Sennaroglu A, Pollock C R and Nathel H 1994 *IEEE J. Quantum Electron.* **30** 1851
- [8] Liu X, Qian L J and Wise F W 1997 *Opt. Commun.* **144** 265
- [9] Yanovsky V P and Wise F W 1994 *Opt. Lett.* **19** 1952
- [10] Zhou B B, Zhang Y D, Zhong X and Wei Z Y 2008 *Chin. Phys. Lett.* **25** 3679
- [11] Agnesi A, Piccinini E and Reali G C 1997 *Opt. Commun.* **135** 77
- [12] Kogelnik H W, Ippen E P, Dienes A and Shank C V 1972 *IEEE J. Quantum Electron.* **8** 373
- [13] Thomann I, Hollberg L, Diddams S A and Equall R 2003 *Appl. Opt.* **42** 1661
- [14] Akhmanov S A, Vysloukh V A and Chirkin A S 1992 *Opt. Femtosecond Laser Pulses* (New York: American Institute of Physics)
- [15] Nebel A, Fallnich C, Beigang R and Wallenstein R 1993 *J. Opt. Soc. Am. B* **10** 2195
- [16] Mokhtari A, Fini L and Chesnoy J 1987 *Opt. Commun.* **61** 421
- [17] Liu T M, Tai S P and Sun C K 2001 *Appl. Opt.* **40** 1957